Isotope effect on the superconducting critical temperature of cuprates in the presence of charge order

Andrés Greco[1,3] and Roland Zeyher[2]

[1] Departamento de Física, Facultad de Ciencas Exactas e Ingeniería and IFIR(UNR-CONICET), Boulevard 27 de Febrero 210 bis, 2000 Rosario, Argentina
[2] Max-Planck-Institut für Festkörperforschung, Heisenbergstrasse 1, D-70569 Stuttgart, Germany

E-mail: agreco@fceia.unr.edu.ar and R.Zeyher@fkf.mpg.de

CrossMark

Abstract

Using the large-N limit of the t–J model and also allowing for phonons and the electron–phonon interaction, we study the isotope effect α for coupling constants appropriate for $YB_2C_3O_y$. We find that α has a minimum at optimal doping and increases strongly (slightly) towards the underdoped (overdoped) region. Using values for the electron–phonon interaction from the local density approximation we get good agreement for α as a function of T_c and doping δ with recent experimental data in $YB_2C_3O_y$. Our results strongly suggest that the large increase of α in the underdoped region is (a) caused by the shift of electronic spectral density from low to high energies associated with a competing phase (in our case a charge density wave) and the formation of a gap, and (b) compatible with the small electron–phonon coupling constants obtained from the local density approximation. We propose a similar explanation for the anomalous behavior of α in Sr-doped La_2CuO_4 near the doping 1/8.

Keywords: phonons, cuprates superconductors, pseudogap regime

(Some figures may appear in colour only in the online journal)

1. Introduction

The isotope effect on the superconducting transition temperature T_c is one of the hallmarks of phonon-induced superconductivity in conventional superconductors [1]. Many experiments showed that the measured isotope coefficient α in these systems is near the theoretical value of 1/2, confirming the important role played by phonons [2]. The isotope effect in high-T_c oxides differs from that in conventional superconductors [3, 4]. Similar to T_c, α depends strongly on doping in this case. At optimal doping, i.e., where T_c assumes

[3] Author to whom any correspondence should be addressed.

its largest value, α turns out to be very small and of the order of 0.05. Decreasing the doping, T_c decreases and vanishes near the onset of long-range antiferromagnetism. At the same time α increases monotonically, reaching low doping values of about 1. Increasing the doping from its optimal value, T_c decreases monotonically down to zero. The behavior of α in this region is presently not as clear as in the underdoped region but seems to be constant or slightly increasing with doping [3, 4]. The above characterization of α applies in particular to the well-investigated Y- and Bi-based high-T_c oxides. The situation in Sr-doped La_2CuO_4 (LSCO) is somewhat different. Large values of α occur near the doping 1/8, where T_c is suppressed [5, 6].

A nonzero isotope coefficient proves the involvement of phonons and the electron–phonon (EP) interaction in the superconducting state. Since α assumes values near 1 in high-T_c oxides, i.e., values which are larger than in all conventional superconductors, it has been concluded [3, 7, 8] that phonons

play an important role in the high-T_c phenomenon. As a result, theories with a strong EP coupling and polarons have been used to explain the observed α [9–11]. On the other hand the experiments show that very large values of α occur in high-T_c oxides if a competing phase with a gap or pseudogap is present [4]. Theories of this kind [12, 13] may explain α without assuming a strong EP coupling. Whether the EP coupling is strong or not in cuprates is of fundamental interest. Angle-resolved photoemission spectra show large electronic self-energies [14, 15], but it is not easy to decide whether they are caused by a strong coupling to phonons [16] or to spin excitations [17]. α, however, is only sensitive to phonons and not to spin excitations. A convincing explanation of α thus could also contribute to the presently controversial discussed question of the role played by phonons in high-T_c oxides.

In this paper we show that the theory of [13] may explain the recently reported doping behavior of α in YBa$_2$Cu$_3$O$_y$ (YBCO) [18]. For this aim we review part of our theory and give new expressions and discussions for α. In our scenario the large increase in α in the underdoped regime can be explained in the presence of a d charge-density wave (CDW) state using small EP interaction constants, as calculated in the local density approximation (LDA) [19–21].

2. Derivation of the expression for α

Our calculation of α is based on the Hamiltonian $H^{t-J} + H^{ep}$, where H^{t-J} is the t–J model and H^{ep} represents the EP interaction. H^{t-J} is given by,

$$H^{t-J} = -\sum_{i,j,\sigma} t_{ij}\tilde{c}_{i\sigma}^{\dagger}\tilde{c}_{j\sigma} + J\sum_{<i,j>}\left(\vec{S}_i \cdot \vec{S}_j - \frac{1}{4}n_i n_j\right) + V_c \sum_{<i,j>} n_i n_j. \quad (1)$$

$t_{ij} = t$ (t') is the hopping integral between the first (second) nearest-neighbor sites on a square lattice; J and V_c are the exchange interaction and the Coulomb repulsion, respectively, between nearest-neighbor sites. $\tilde{c}_{i\sigma}^{\dagger}$ and $\tilde{c}_{i\sigma}$ are creation and annihilation operators for electrons with spin σ ($\sigma = \downarrow, \uparrow$), respectively, excluding double occupancies of sites. $n_i = \sum_{\sigma} \tilde{c}_{i\sigma}^{\dagger}\tilde{c}_{i\sigma}$ is the electron density and $\vec{S}_i$ the spin operator. $<i, j>$ denotes a sum over pairs of sites i and j.

In the framework of the large-N expansion, the spin index σ in (1) is extended to N components, the coupling constants scaled as $t \to 2t/N$, $t' \to 2t'/N$, $J \to 2J/N$, and $V_c \to 2V_c/N$, and the large N limit is considered [22]. As a result, the quasiparticle dispersion is given by $\epsilon(\mathbf{k}) = -2(t\delta + rJ)(\cos(k_x) + \cos(k_y)) - 4t'\delta \cos(k_x)\cos(k_y) - \mu$, where $r = 1/N_s \sum_{\mathbf{q}} \cos(q_x) f(\epsilon(\mathbf{q}))$. f is the Fermi function, δ the doping away from half-filling, μ the chemical potential, and N_s the number of sites. In the following we use the lattice constant a and t as length and energy units, respectively. In addition, we take $t'/t = -0.35$ and $J/t = 0.3$, which are typical values for cuprates.
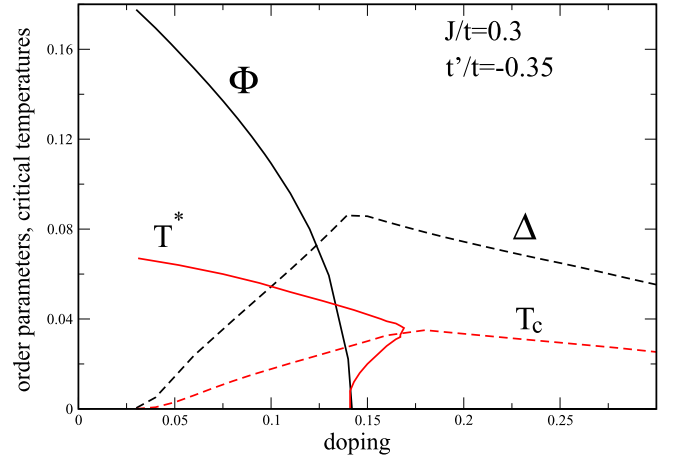

Figure 1. Zero-temperature order parameters Φ and Δ and the critical temperatures T^* and T_c as a function of doping.

As discussed previously [22] the above model shows instabilities with respect to a d CDW [23, 24] and a superconducting phase. The corresponding order parameters are

$$i\Phi(\mathbf{k}) = -4J\gamma(\mathbf{k})\frac{T}{N_s}\sum_{\mathbf{k}',n}\gamma(\mathbf{k}')g_{13}(\mathbf{k}', i\omega_n) \quad (2)$$

and

$$\Delta(\mathbf{k}) = -4\tilde{J}\gamma(\mathbf{k})\frac{T}{N_s}\sum_{\mathbf{k}',n}\gamma(\mathbf{k}')g_{12}(\mathbf{k}', i\omega_n). \quad (3)$$

T is the temperature and $i\omega_n$ a fermionic Matsubara frequency. g_{12} and g_{13} are the elements (1,2) and (1,3), respectively, of the 4×4 Green's function

$$g^{-1}(i\omega_n, \mathbf{k}) = \begin{pmatrix} i\omega_n - \epsilon(\mathbf{k}) & -\Delta(\mathbf{k}) & -i\Phi(\mathbf{k}) & 0 \\ -\Delta(\mathbf{k}) & i\omega_n + \epsilon(\mathbf{k}) & 0 & i\Phi(\bar{\mathbf{k}}) \\ i\Phi(\mathbf{k}) & 0 & i\omega_n - \epsilon(\bar{\mathbf{k}}) & -\Delta(\bar{\mathbf{k}}) \\ 0 & -i\Phi(\bar{\mathbf{k}}) & -\Delta(\bar{\mathbf{k}}) & i\omega_n + \epsilon(\bar{\mathbf{k}}) \end{pmatrix} \quad (4)$$

with the abbreviation $\bar{\mathbf{k}} = \mathbf{k} - \mathbf{Q}$, where $\mathbf{Q} = (\pi, \pi)$ is the wave vector of the CDW. In (2) and (3) we have used the fact that the most stable solutions for $\Delta(\mathbf{k})$ and $\Phi(\mathbf{k})$ have d-wave symmetry; i.e., $\Delta(\mathbf{k}) = \Delta\gamma(\mathbf{k})$, and $\Phi(\mathbf{k}) = \Phi\gamma(\mathbf{k})$ with $\gamma(\mathbf{k}) = (\cos(k_x) - \cos(k_y))/2$. In (3) $\tilde{J} = J - V_c$, where we have introduced a Coulomb repulsion $V_c = 0.2J$ between nearest-neighbor sites to prevent an instability of the CDW phase towards phase separation at low doping.

For convenience we have reproduced in figure 1 previous results [13] for Φ and Δ at $T = 0$, and for T_c and T^*, as a function of doping. T^* is the temperature where the CDW phase develops. The phase diagram is qualitatively similar to the experiments; i.e., there is a dome-like behavior for T_c with a maximum value around $\delta \sim 0.16$ where the CDW appears. Similarly as in experiments [25, 26], Φ and Δ compete and coexist with each other at low temperatures. Using $t = 400$ meV, the resulting values for T_c and T^* compare well with the experimental ones.

Next we discuss the phonon-induced interaction H^{ep} between electrons, which can be written in the static limit as,

$$H^{ep} = -\frac{1}{2}\sum_{\mathbf{k},\mathbf{k}',\mathbf{k}'',\mathbf{k}''',\sigma,\sigma'}' V(\mathbf{k}-\mathbf{k}')\tilde{c}^{\dagger}_{\mathbf{k}\sigma}\tilde{c}_{\mathbf{k}'\sigma}\tilde{c}^{\dagger}_{\mathbf{k}''\sigma'}\tilde{c}_{\mathbf{k}'''\sigma'}. \quad (5)$$

The prime at the summation sign means that $\mathbf{k}-\mathbf{k}'+\mathbf{k}''-\mathbf{k}'''$ must be equal to a reciprocal lattice vector. In the following the d-wave part of $V(\mathbf{k}-\mathbf{k}')$ will be important. It is obtained by replacing $V(\mathbf{k}-\mathbf{k}')$ by $4V\gamma(\mathbf{k})\gamma(\mathbf{k}')$ which defines the d-wave coupling constant V for a phonon-induced nearest-neighbor interaction.

An expression for α has been given in [13]. There it has also been shown that two simplifications can be made without changing the results much. First, one may neglect the influence of phonons on T^*. Secondly, the EP interaction yields a contribution to the pairing but also one to the quasi-particle weight Z. If the general question is studied of whether phonons increase or decrease T_c, both effects are present and compete with each other. Numerical calculations indicate that generically the second effect dominates so that T_c decreases [27]. Our aim, however, is not to determine the change in T_c when the EP interaction is turned on but when the ionic mass M is changed. Writing $Z = 1 + \lambda_s$, it is well known that the dimensionless EP coupling constant in the s-wave channel, λ_s, is independent of M. The same is then true also for Z. Since there is good evidence that the EP coupling in cuprates is rather small [21], we may even use in the following the approximation $Z = 1$.

Introducing a phonon cutoff ω_0 and the cutoff function $\Theta_n(\omega_0 - |\omega_n|)$, the gap equation reads

$$\Delta(\mathbf{k}, i\omega_n) = -4\tilde{J}\gamma(\mathbf{k})\frac{T}{N_s}\sum_{\mathbf{k}',n'}\gamma(\mathbf{k}')g_{12}(\mathbf{k}', i\omega_{n'})$$
$$- 4V\gamma(\mathbf{k})\Theta_n\frac{T}{N_s}\sum_{\mathbf{k}',n'}\Theta_{n'}\gamma(\mathbf{k}')g_{12}(\mathbf{k}', i\omega_{n'}). \quad (6)$$

The condition for T_c can be written as,

$$(1 + F_{11})(1 + F_{22}) - F_{12}^2 = 0 \quad (7)$$

where

$$F_{11} = -2\tilde{J}\int_0^\infty d\omega \frac{N_d(\omega)}{\omega}\tanh\left(\frac{\omega}{2T_c}\right), \quad (8)$$

$$F_{12} = -2\sqrt{\tilde{J}V}\int_0^\infty d\omega \frac{N_d(\omega)}{\omega}\frac{2}{\pi}$$
$$\cdot Im\left[\psi\left(\frac{1}{2} + \frac{i\omega}{2\pi T_c}\right) - \psi\left(\frac{\omega_0}{2\pi T_c} + 1 + \frac{i\omega}{2\pi T_c}\right)\right], \quad (9)$$

$F_{22} = \sqrt{V/\tilde{J}}F_{12}$, and ψ is the digamma function. The d-wave projected density of electronic states is given by

$$N_d(\omega) = \frac{1}{N_s}\sum_{\mathbf{k}}\gamma^2(\mathbf{k})\sum_{\alpha=1}^2\frac{E_\alpha^2(\mathbf{k}) - \epsilon^2(\bar{\mathbf{k}}) - \Phi^2(\mathbf{k})}{E_\alpha^2(\mathbf{k}) - E_{\bar{\alpha}}^2(\mathbf{k})}$$
$$\cdot\left(\delta(\omega - E_\alpha(\mathbf{k})) + \delta(\omega + E_\alpha(\mathbf{k}))\right), \quad (10)$$
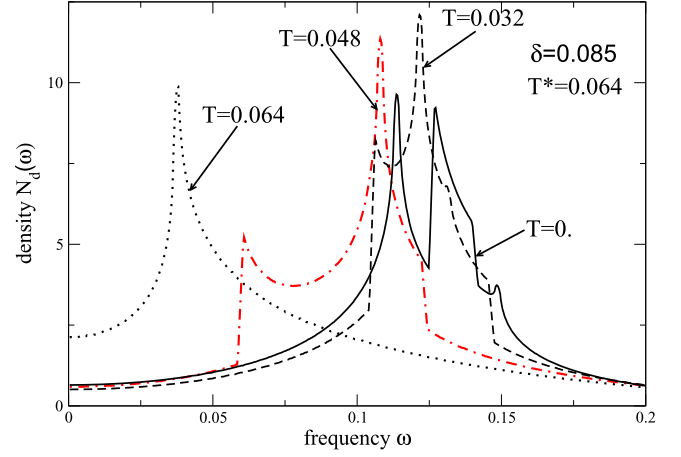

Figure 2. Density $N_d(\omega)$ for doping $\delta = 0.085$ and several temperatures as a function of frequency ω.

with $\bar{\alpha} = 3 - \alpha$, and

$$E_{1,2} = \epsilon_+(\mathbf{k}) \pm \sqrt{\epsilon_-^2(\mathbf{k}) + \Phi^2(\mathbf{k})} \quad (11)$$

with $\epsilon_\pm = (\epsilon(\mathbf{k}) \pm \epsilon(\bar{\mathbf{k}}))/2$.

Figure 2 shows $N_d(\omega)$ as a function of ω for the doping $\delta = 0.085$ and several temperatures T. For $T \geqslant T^*$ the density is dominated by a sharp peak at about $\omega \sim 0.04$, corresponding to the van Hove peak in the normal state. Decreasing T, this single peak splits into two peaks; both move towards higher energies and come closer to each other. This behavior can be understood by noting that the main contribution in the sum over $\mathbf{k}$ comes from the surroundings of the X-point. Then the first term under the square root in (11) is in general much smaller than the second one, and the square root may be expanded, yielding for positive energies

$$E_{1,2} \rightarrow \epsilon_+(\mathbf{k}) + \Phi(\mathbf{k}) \pm \frac{\epsilon_-^2(\mathbf{k})}{\Phi(\mathbf{k})}. \quad (12)$$

Thus one expects that $N_d(\omega)$ shows a doublet with a mean energy $\epsilon_+(\mathbf{k}) + \Phi(\mathbf{k})$ and a splitting energy $2\epsilon_-^2(\mathbf{k})/\Phi(\mathbf{k})$. With increasing Φ the splitting decreases in agreement with the curves in figure 2.

The isotope coefficient α is defined by

$$\alpha = \frac{\omega_0}{2T_c}\frac{\partial T_c}{\partial \omega_0}. \quad (13)$$

From (7) follows then

$$\alpha = -\frac{\omega_0}{2T_c}\frac{F' \cdot \frac{\partial F_{12}}{\partial \omega_0}}{\frac{\partial F_{11}}{\partial T_c}(1 + F_{22}) + F' \cdot \frac{\partial F_{12}}{\partial T_c}}, \quad (14)$$

with

$$F' = (1 + F_{11})\sqrt{V/\tilde{J}} - 2F_{12}. \quad (15)$$

For a weak EP coupling constant V, α reduces to

$$\alpha = \frac{\omega_0}{T_c}\frac{F_{12}\partial F_{12}/\partial \omega_0}{\partial F_{11}/\partial T_c}, \quad (16)$$
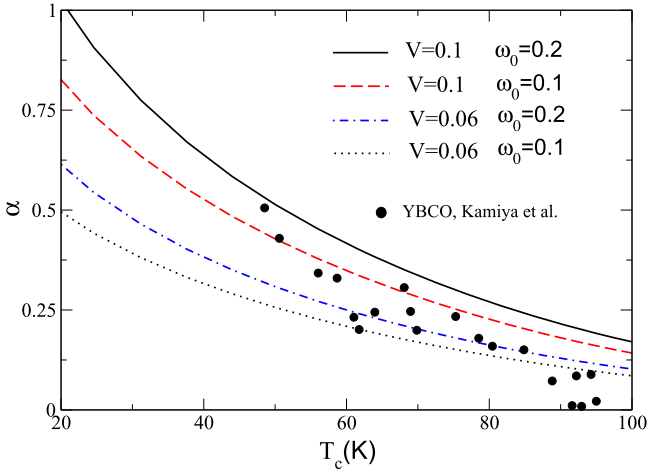
in agreement with (18) of [13].

Figure 3. Isotope coefficient α as a function of T_c for different EP couplings V and phonon frequencies ω_0. The filled circles are experimental points from [18].
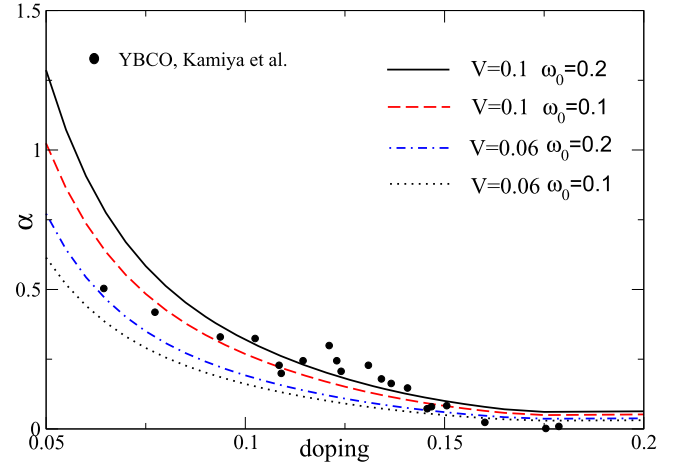

Figure 4. Isotope coefficient α as a function of doping δ for the same parameters as in figure 3. The filled circles are experimental points from [18].

3. Results and discussion

3.1. YBCO

Figures 3 and 4 show α versus T_c and δ, respectively, for $V = 0.06$ and $V = 0.10$, and two phonon frequencies. $\omega_0 = 0.1$ and 0.2 corresponds to the buckling and half-breathing phonon modes in YBCO. The solid points are experimental results from [18]. They all lie in the region between the curves calculated with parameter values representative for cuprates. The above choice of parameter values for phonons is, of course, unproblematic. More controversial may be the employed values for the EP coupling constants. First principles calculations of total EP constants have been described in [21]. The results are given in terms of dimensionless coupling constants λ_s and λ_d for the s- and d-wave channel, respectively. For each channel, λ and V are related by $\lambda = VN(0)$, where $N(0)$ is the density of electronic states at the Fermi energy in the corresponding symmetry channel. LDA calculations yield for YBa$_2$Cu$_3$O$_7$ $\lambda_s \sim 0.24$ and $\lambda_d \sim 0.022$ [21]. These values are rather small, particularly, the value for λ_d. On the other hand there is good evidence from several experiments that such small values are not unreasonable: Angle-resolved photoemission data in LSCO [15, 28] yielded $\lambda_s \sim 0.4$. Similarly, superconductivity-induced shifts of zone center phonons are in good agreement with calculated LDA values [29, 30] and therefore with such small EP coupling constants. In figures 3 and 4 only EP coupling constants in the d-wave channel enter, for which we used $V = 0.06$ and 0.10, which are slightly larger than the LDA values. They describe the experimental points somewhat better than the bare LDA values. One should keep in mind that such adjustments (from $\lambda_d \sim 0.02$ to $\lambda_d \sim 0.04$) should be considered as minor, because we always stay in the region of very small EP couplings.

It is worth remarking that the observed increase of α in the underdoped region of YBCO can be quantitatively explained not only by employing such small values for the EP

coupling constants but by noting that a reasonable agreement between experiment and theory requires them. As discussed above the large isotope effect found in underdoped cuprates has been interpreted as evidence for a strong EP coupling in these systems. From the above analysis the conclusion is quite different: The large observed isotope shifts in underdoped cuprates are the result of a competition of superconductivity with another ground state which produces the pseudogap. They can be explained using the small d-wave EP coupling constant obtained in the LDA calculations. Figures 3 and 4 demonstrate this for the case of a d CDW state as a competing state, but we expect similar results for other ground states, as long as they are associated with a gap or a pseudogap.

The above calculations indicate that a pseudogap and the associated shift of the density of states from low to high energies are responsible for the strong increase of α in the underdoped regime. It is, however, clear that a reduction of $N_d(0)$ alone cannot increase α as long as $N_d(\omega)$ is constant on the scale of ω_0. It is therefore interesting to analyze the above equations in more detail and to find out what exactly causes the increase in α. For the following analytical results we will assume that the density of states $N_d(\omega)$ can be considered either as constant or that T_c is sufficiently low; i.e., we will consider the overdoped or the strongly underdoped regions. It also will be sufficient to consider the expression (16) for α, which is valid for a weak EP coupling.

The derivative in the denominator of (16) may be approximated as

$$\frac{\partial F_{11}}{\partial T_c} = \frac{\tilde{J}}{T_c} \int_0^\infty d\epsilon \frac{N_d(2\epsilon T_c)}{\cosh^2(\epsilon)} \approx \frac{\tilde{J}}{T_c} N_d(0). \tag{17}$$

The term F_{12} can be written as

$$F_{12} = -2\sqrt{V\tilde{J}} \int_0^\infty d\epsilon N_d(\epsilon) \left[T_c \sum_n \frac{1}{\omega_n^2 + \epsilon^2} \right.$$

$$\left. - T_c \sum_{|\omega_n| > \omega_0} \frac{1}{\omega_n^2 + \epsilon^2} \right]. \tag{18}$$

Let us write F_{12} as

$$F_{12} = \sqrt{V\tilde{J}}\left(F_{12}^{(1)} + F_{12}^{(2)}\right), \qquad (19)$$

with

$$F_{12}^{(1)} = \int_0^{\omega_0} d\epsilon \frac{N_d(\epsilon)}{\epsilon} \tanh\left(\frac{\epsilon}{2T_c}\right), \qquad (20)$$

$$F_{12}^{(2)} = \int_{\omega_0}^{\infty} d\epsilon \frac{N_d(\epsilon)}{\epsilon} \tanh\left(\frac{\epsilon}{2T_c}\right)$$
$$- \int_0^{\infty} \frac{N_d(\epsilon)}{\omega_0} \arctan\left(\frac{\omega_0}{\epsilon}\right). \qquad (21)$$

In the last term in (21) the zero-temperature limit has been taken. The derivative $\frac{\partial F_{12}}{\partial \omega_0}$ acts only on the last term in $F_{12}^{(2)}$, yielding

$$\frac{\partial F_{12}^{(2)}}{\partial \omega_0} = -\int_0^{\infty} d\epsilon \frac{N_d(\epsilon)}{\omega_0^2 + \epsilon^2}. \qquad (22)$$

Inserting the above results into (16) gives

$$\alpha = -\frac{\omega_0 V}{N_d(0)} \frac{F_{12}}{\sqrt{V\tilde{J}}} \int_0^{\infty} d\epsilon \frac{N_d(\epsilon)}{\omega_0^2 + \epsilon^2}. \qquad (23)$$

Numerical evaluation of (18) shows that F_{12} is practically constant as a function of doping above optimal doping and only very slowly increasing towards lower dopings. Thus we may consider F_{12} in (23) as a constant. As a result we obtain for the increase of α relative to its value α_0 at optimal doping, i.e., at the onset of the CDW,

$$\alpha\big/\alpha_0 = \frac{2}{\pi} \int_0^{\infty} d\epsilon \frac{\omega_0}{\omega_0^2 + \epsilon^2} \cdot \frac{N_d(\epsilon)}{N_d(0)}. \qquad (24)$$

The above formula allows us to understand the large increase of α in the underdoped regime. Near optimal doping $N(\epsilon)$ depends only weakly on frequency so that the density ratio $N_d(\omega)/N_d(0)$ and, therefore, also α/α_0 is near 1. Below optimal doping the spectral weight is shifted from low to high frequencies, which produces the pseudogap. As a result the ratio $N_d(\omega)/N_d(0)$ is large around the pseudogap, leading to large values for α/α_0. Since $N_d(0)$ is roughly proportional to δ, α/α_0 increases monotonically with decreasing doping, yielding values which may exceed by far the canonical BCS value of 1/2. Taking the limit $\omega_0 \to 0$ in (24), the first factor under the integral becomes a delta function, and we obtain $\alpha/\alpha_0 = 1$. The absence of an enhancement of α for small ω_0 can easily be understood: The main part in the integral in (24) comes from the region of small ϵ, well below the pseudogap, where $N_d(0)$ is small. The contribution from electronic spectral density shifted to the frequency region around the gap is missing, and no substantial enhancement of α can occur. This case also shows that the reduction of $N_d(0)$ due to the formation of the gap does not cause an increase of α by itself. Instead the shift of spectral weight from low to high frequencies near the pseudogap is responsible for the increase of α. For large phonon frequencies, α/α_0 decreases with increasing ω_0. Thus one expects that α/α_0 as a function of ω_0 first increases, passes then through a maximum, and finally
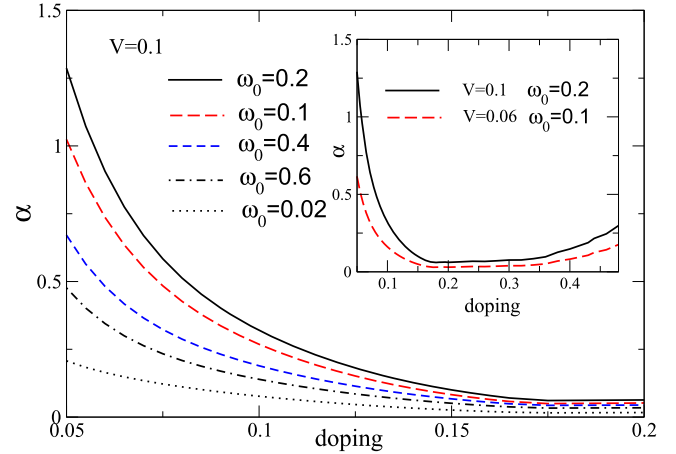

Figure 5. Isotope coefficient α as a function of doping for $V = 0.1$ and several phonon frequencies ω_0, demonstrating the nonmonotonic dependence of α on ω_0. Inset: α over a larger doping region.

decreases. The curves in figure 5, calculated with the full expressions for the functions F, illustrate nicely this behavior.

In the overdoped region one may assume that the density of states $N_d(\epsilon)$ is constant. The approximations leading to (24) imply then $\alpha = \alpha_0$ throughout the overdoped region. A better approximation in this region is obtained by using ω_0 as the cutoff in the energy integration in F_{12}. The two terms in $F_{12}^{(2)}$ cancel then exactly, and $F_{12}^{(1)}$ can be evaluated as in the usual BCS theory, yielding,

$$\alpha = \frac{\pi\lambda_d}{2} \log\left(\frac{1.14\omega_0}{T_c}\right). \qquad (25)$$

A similar result has been first derived in [31]. For optimal doping where T_c is highest, α shows a minimum with a value which for $T_c > 1.14\omega_0$ is weakly negative. For more realistic parameter values the logarithmic factor is about 1, and thus $\alpha \approx \lambda_d$. The observed small values $\alpha_0 \sim 0.05$ in cuprates with the highest T_c do require similar values for λ_d in good agreement with the values obtained from the LDA calculations. Our analytical expressions for α in the under- and overdoped region used ω_0 as a cutoff, but one time along the imaginary and one time along the real axis. Taking the cutoff always along the real axis is not suitable in the underdoped region, because if the density peak in $N_d(\omega)$ coincides with the phonon frequency, one obtains a spurious peak in the curve α versus δ. Using the cutoff along the imaginary axis we never found such an artifact and therefore used this choice of cutoff in all our numerical calculations.

The inset of figure 5 shows α versus δ, calculated without approximations, over a large doping region. In the overdoped region this function increases roughly as predicted by (25). A closer look reveals, however, that both the analytic expressions (24) for the underdoped regime and, to a lesser degree, (25) for the overdoped regime do not well agree with the numerically evaluated curves. One reason is that our model $N_d(\omega)$ in equation (17) varies in the energy interval $[0, 2T_c]$ considerably so that the approximation proposed in that equation is problematic. Band structure effects thus play a role in our model, even at low energies, producing
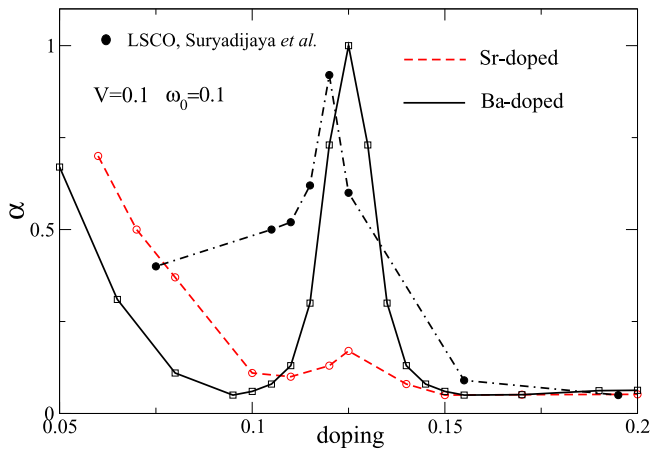
Figure 6. Isotope coefficient α as a function of doping. Filled circles are experimental points in LSCO from [5]. Empty circles and squares are calculated values for $La_{2-x}Ba_xCuO_4$ and LSCO, respectively. Corresponding points have been joined smoothly by lines.

fluctuations in the curve α versus δ if calculated with (24). In the numerically exact calculated curves in figures 3–5, such fluctuations are absent due to a properly carried out energy integration in (17). Though (24) and (25) are thus not suitable to obtain accurate values, they nevertheless explain correctly the curves α versus δ at low and high dopings.

3.2. La- and Ba-doped La_2CuO_4

Our theory can also be applied to Sr- and Ba- doped La_2CuO_4. $La_{2-x}Ba_xCuO_4$ shows a variety of phase transitions near the doping $\delta = 1/8$ [32]. T_c exhibits a dip between $\delta_1 = 0.155$ and $\delta_2 = 0.095$, which nearly touches zero at $\delta = 0.125$ [32, 33]. Between these limiting dopings a leading-phase CO with charge stripe order extends towards higher temperatures above the superconducting phase in a domelike manner, touching T_c at the end points. There are additional phases of spin stripe order or of orthorhombic or tetragonal symmetry present, which will be disregarded in the following. Above δ_1 or below δ_2, T_c is decreasing with increasing distance from these points, reaching very small values near $\delta = 0.25$ and 0.05, respectively. The phase diagram of the sister compound LSCO does not contain long-ranged phases around the doping 1/8. Nevertheless it is probable that superconductivity competes with phases in the particle–hole channel near this doping, because T_c shows a pronounced dip in this region [5, 6]. Also angle resolved photoemission experiments find in LSCO a pseudogap that sets in at around $\delta = 0.20$, and exists and increases in magnitude towards lower dopings. The isotope coefficient in LSCO (see figure 6) is very small at the large doping value of 0.20, where the pseudogap forms. With decreasing δ, α first increases slightly and then very rapidly, reaching a maximum near the doping 1/8 with a value of about 1. Decreasing δ further, α decreases but settles down in the region of about 0.5.

In view of the above phase diagrams and the behavior of α in LSCO, it is natural to assume that the doping dependence

of T_c and α are caused by gaps or pseudogaps similar to those in YBCO. In order to transfer our results from YBCO to $La_{2-x}Ba_xCuO_4$ and LSCO, we consider the calculated α in YBCO as a function of $T_c/T_{c,0}$, where $T_{c,0}$ is the optimal T_c for a doping near the onset of the pseudogap. Treating first $La_{2-x}Ba_xCuO_4$, we can read off from figure 2 of [33] the doping as a function of $T_c/T_{c,0}$, where $T_{c,0}$ is the value of T_c near the dopings δ_1 or δ_2. Identifying the two ratios for the reduction of T_c, one obtains α as a function of doping in $La_{2-x}Ba_xCuO_4$. The same procedure can be applied to LSCO. From figure 3 in [6] one can read off δ as a function of $T_c/T_{c,0}$, where $T_{c,0}$ is the largest transition temperature near $\delta = 0.15$. Comparing this reduction ratio with the case of YBCO, one finds the doping dependence of α in LSCO. Figure 6 contains the obtained curves, calculated for $V = 0.1$ and $\omega_0 = 0.1$, together with experimental values for LSCO from [5]. Our calculation suggests the following interpretation of the experimental α in LSCO. One has to distinguish between two pseudogaps in LSCO. The first one is the usual pseudogap, which is observed by angle-resolved photoemission and which exists below $\delta \sim 0.20$ [34]. This pseudogap corresponds to that occurring in underdoped cuprates and develops at T^*. At low doping, superconductivity competes with the phase underlying the pseudogap, leading to the overall decrease of T_c down to very low values near $\delta = 0.05$. At the same time this decrease of T_c is associated with a monotonic increase of α similar to that in YBCO. The second pseudogap is located between $\delta = 0.10$ and $\delta = 0.15$ and is due to static (in $La_{2-x}Ba_xCuO_4$) or fluctuating (in LSCO) stripes. As a result T_c is strongly (in $La_{2-x}Ba_xCuO_4$) or slightly (in LSCO) suppressed. Correspondingly, the increase of α in figure 6 is large for the Ba- and small for the Sr- doped systems. It is interesting to see that the calculated curve for LSCO shows only a small peak at doping 1/8, quite in contrast to the experimental curve. The reason for this is that the employed experimental T_c curve exhibits only a small dip near the doping 1/8. One prediction of our calculation is that α in Ba-doped La_2CuO_4 should show a large peak near doping 1/8. Though our calculation for α in LSCO is not able to get quantitative agreement with experiment, we think that the shift of the spectral weight from low to higher energies associated with the formation of the pseudogap plays also a role in LSCO.

Finally we would like to mention that strong renormalizations (softenings and broadenings) of phonons have been observed in underdoped cuprates (see [35] and references therein). These anomalies occur for wave vectors along the crystalline axis with a length of about 0.3 and are seen both in acoustical [36] and optical bond-stretching phonons [37]. They are probably related to the recently observed charge order in these systems [36]. On the other hand, extensive LDA calculations, performed for $YBa_2Cu_3O_7$, did not yield unusual softenings [21, 38] and cannot explain these phonon anomalies. However, our main result is independent of the validity of the LDA in cuprates and shows only that the observed large values of α in underdoped cuprates are at least compatible with the LDA values for the EP coupling constants. The existence of the above phonon anomalies suggests

that it is not possible to conclude quite generally from these and other successful LDA results [29, 30] that the EP coupling is necessarily small in the cuprates. Thus, the correct explanation of the phonon anomalies is presently an open problem and beyond the scope of our paper, similarly to their influence on T_c.

4. Conclusions

In summary, our calculations of the isotope coefficient α were based on a mean-field, like treatment of the t–J model, where optimal doping coincides with the onset of a CDW, which competes with superconductivity in the underdoped regime and suppresses T_c there. Adding phonons and the EP coupling, our model can explain the strong experimental increase of α in the underdoped region, using at the same time the small EP coupling constants from the LDA. Thus we conclude that the large values for α in the underdoped regime give no evidence for a large EP coupling in these systems but are compatible with the small LDA values once the competing phase is taken into account. Large enhancements of α are found if the phonon energy ω_0 and the gap Φ are comparable in magnitude and are absent for very small or large ratios ω_0/Φ. Our explanation of the behavior of α is supported by several experimental facts: α assumes its minimum at optimal doping, where the competing phase sets in, and strongly increases towards lower dopings in the presence of the competing phase; in this region superconductivity forms from a state where the density of electronic states varies strongly over the scale of phonon energies, which is quite different from the normal state. All these features make, in our opinion, explanations very improbable that are based on a strong EP interaction, polarons, or anharmonic mechanisms.

Acknowledgments

References

[1] Reynolds C A, Serin B, Wright W H and Nesbitt L B 1950 *Phys. Rev.* **78** 487
[2] Parks R D 1969 *Superconductivity* vol I and II (New York: Marcel Dekker)
[3] Franck J P 1994 Experimental studies of the isotope effect in high temperature superconductors *Physical Properties of High Temperature Superconductors IV* ed D M Ginsberg (Singapore: World Scientific) ch 4, pp 189–293
[4] Pringle D J, Williams G V M and Tallon J L 2000 *Phys. Rev.* B **62** 12527–33
[5] Suryadijaya, Sasagawa T and Takagi H 2005 *Physica* C **426431** 402–6
[6] Takagi H, Ido T, Ishibashi S, Uota M, Uchida S and Tokura Y 1989 *Phys. Rev.* B **40** 2254–61
[7] Bornemann H J and Morris D E 1991 *Phys. Rev.* B **44** 5322–5
[8] Keller H 2005 Unconventional isotope effects in cuprate superconductors *Superconductivity in Complex Systems* (*Structure and Bonding* vol 114) ed K Müller and A Bussmann-Holder (Heidelberg: Springer) 143–69
[9] Kornilovitch P E and Alexandrov A S 2004 *Phys. Rev.* B **70** 224511
[10] Macridin A and Jarrell M 2009 *Phys. Rev.* B **79** 104517
[11] Bussmann-Holder A, Keller H, Bishop A R, Simon A, Micnas R and Müller K A 2005 *Europhys. Lett.* **72** 423
[12] Dahm T 2000 *Phys. Rev.* B **61** 6381–6
[13] Zeyher R and Greco A 2009 *Phys. Rev.* B **80** 064519
[14] Zhou X J et al 2005 *Phys. Rev. Lett.* **95** 117001
[15] Park S R, Cao Y, Wang Q, Fujita M, Yamada K, Mo S K, Dessau D S and Reznik D 2013 *Phys. Rev.* B **88** 220503
[16] Lanzara A et al 2001 *Nature* **412** 510–4
[17] Manske D, Eremin I and Bennemann K H 2001 *Phys. Rev. Lett.* **87** 177005
[18] Kamiya K, Masui T, Tajima S, Bando H and Aiura Y 2014 *Phys. Rev.* B **89** 060505
[19] Heid R, Bohnen K P, Zeyher R and Manske D 2008 *Phys. Rev. Lett.* **100** 137001
[20] Giustino F, Cohen Marvin L and Louie Steven G 2008 *Nature* **452** 975–8
[21] Heid R, Zeyher R, Manske D and Bohnen K P 2009 *Phys. Rev.* B **80** 024507
[22] Cappelluti E and Zeyher R 1999 *Phys. Rev.* B **59** 6475–86
[23] Hsu T C, Marston J B and Affleck I 1991 *Phys. Rev.* B **43** 2866–77
[24] Chakravarty S, Laughlin R B, Morr D K and Nayak C 2001 *Phys. Rev.* B **63** 094503
[25] Hüfner S, Hossain M A, Damascelli A and Sawatzky G A 2008 *Rep. Prog. Phys.* **71** 062501
[26] Norman M R, Pines D and Kallin C 2005 *Adv. Phys.* **54** 715–33
[27] Macridin A, Moritz B, Jarrell M and Maier T 2006 *Phys. Rev. Lett.* **97** 056402
[28] Zhao L et al 2011 *Phys. Rev.* B **83** 184515
[29] Friedl B, Thomsen C and Cardona M 1990 *Phys. Rev. Lett.* **65** 915–8
[30] Rodriguez C O, Liechtenstein A I, Mazin I I, Jepsen O, Andersen O K and Methfessel M 1990 *Phys. Rev.* B **42** 2692–5
[31] Daemen L L and Overhauser A W 1990 *Phys. Rev.* B **41** 7182–4
[32] Hücker M, v Zimmermann M, Gu M, Xu G D, Wen Z J, Xu J S, Kang G, Zheludev H J and Tranquada J M A 2011 *Phys. Rev.* B **83** 104506
[33] Moodenbaugh A R, Xu Y, Suenaga M, Folkerts T J and Shelton R N 1988 *Phys. Rev.* B **38** 4596–600
[34] Yoshida T et al 2009 *Phys. Rev. Lett.* **103** 037004
[35] Reznik D, Pintschovius L, Ito M, Iikubo S, Sato M, Goka H, Fujita M, Yamada K, Gu G D and Tranquada J M 2006 *Nature* **440** 1170–3
[36] Le Tacon M, Bosak A, Souliou S M, Dellea G, Loew T, Heid R, Bohnen K-P, Ghiringhelli G, Krisch M and Keimer B 2014 *Nat. Phys.* **10** 52–8
[37] Pintschovius L, Reznik D, Reichardt W, Endoh Y, Hiraka H, Tranquada J M, Uchiyama H, Masui T and Tajima S 2004 *Phys. Rev.* B **69** 214506
[38] Reznik D, Sangiovanni G, Gunnarsson O and Devereaux T P 2008 *Nature* **455** 6–7